Back-to-Back Measurement for Characterization of Phased-Array Antennas

Wei-Chun Chang, Gregory J. Wunsch, and Daniel H. Schaubert, *Fellow, IEEE*

***Abstract*—A back-to-back measurement method for characterizing phased-array antennas is described. The method yields the complex active impedance of an antenna in a large phased array at any desired frequency and scan angle without the need of a feed network to excite the antenna under test. This avoids the cost and de-embedding procedure associated with the feed network. Measurements are performed by using two different transmission networks to connect identical arrays in a back-to-back configuration. The new method is particularly well suited to printed antennas and is illustrated by using tapered-slot antennas. Back-to-back measurements in waveguide simulators compare well to traditional waveguide simulator measurements and measurements in an anechoic chamber compare well to results from computer codes based on full-wave method of moments.**

***Index Terms*—Measurement, notch array, phased array, tapered slot antenna, waveguide simulator.**

I. Introduction

PHASED-array antennas have the ability to scan the main beam without mechanical movement. Free from problems associated with the mass or the inertia of moving parts, phased-array antennas can sweep their beams quickly, tracking multiple targets at the same time and shaping the antenna beams as needed [1]–[4].

The design of large phased arrays usually takes the infinite-array approach in which each radiator is treated as if it is in an infinite-array environment. This facilitates design and analysis since all elements behave alike. Computer-simulations based on the unit cell or measurements of central elements in moderately large arrays yield information about element performance and mutual coupling. However, measurements to characterize array performance are usually limited in their capability to obtain complex impedance information for arbitrary frequencies and scan angles. Waveguide simulators [5]–[8] yield the complex impedance, but only at particular scan and frequency values. Active element patterns [9]–[11] permit characterization at arbitrary scan angles and frequencies, but yield only the magnitude of the reflection coefficient and require matched terminations on a large number of elements. A fully driven array with some form of impedance measurement is needed to obtain complex impedance at all scan angles and frequencies. The cost of a full array system rises sharply when the number of radiating elements gets large, especially in wide-band cases. This is mainly due to the wide-band power dividers, phase shifters, and connectors used in the feed networks. The cost for radiators usually remains relatively low. Furthermore, the feed networks used in the testing stage may differ from those used in the final design. This calls for de-embedding procedures, which generally are not trivial. For these reasons, the use of feed networks in the design and test stage is extra cost and complexity that may not be necessary. It is easier to characterize radiators without the cumbersome feed networks.

In this paper, a back-to-back measurement method is described. Using this scheme, the antenna under test can be fabricated in its natural structure without adaptors regardless of the type of the input port on the measurement equipment. phased-array antennas can be characterized at arbitrary scan angle, polarization, and frequency without feed networks. Suggestions for improving upon the basic method are included. Also, a "free-space" measurement validation is presented.

In the next section, the underlying concepts of the new method are introduced. The necessary formula derivations and the measurement setup are presented in that section. Section III demonstrates the results obtained by applying the back-to-back scheme to waveguide simulators and to finite array measurements. They are compared to the results from a one-port waveguide simulator and calculated data from computer codes. The error analysis is discussed in Section IV. This includes a re-examination of the assumptions made in the back-to-back scheme and their impacts on measurement accuracy. This leads to several suggestions to improve the technique.

II. Back-to-Back Measurement

The configuration of the back-to-back measurement is closely related to constrained lens array antennas. The mismatch at feed-through lines has been found to cause problems in the operation of lens array antennas [12], [13]. In the back-to-back scheme, the mismatch is explicitly used to characterize the array antenna. This scheme has not been previously applied to antenna arrays, but it is similar, in principle, to de-embedding S-parameter measurements [14] and de-embedding by division [15]. Those formula derivations resemble the back-to-back measurement derivations of the authors' previous work [16].

In the back-to-back measurement method, the antennas under test are measured in pairs. They are not directly connected to the measurement equipment, which is usually a vector network analyzer (VNA). Instead, a pair of identical antennas are connected back-to-back by a known transmission network to form a "lens" (see Fig. 1). In the case of stripline-fed notch antennas, the transmission network is stripline. As can be seen in Fig. 1,

Manuscript received March 16, 1998; revised March 16, 2000.

W. C. Chang and D. H. Schaubert are with the Department of Electrical and Computer Engineering, University of Massachusetts, Amherst, MA 01003 USA.

G. J. Wunsch is with Sanders, A Lockheed Martin Company, Nashua, NH 03061 USA.

Publisher Item Identifier S 0018-926X(00)06942-8.

0018–926X/00$10.00 © 2000 IEEE

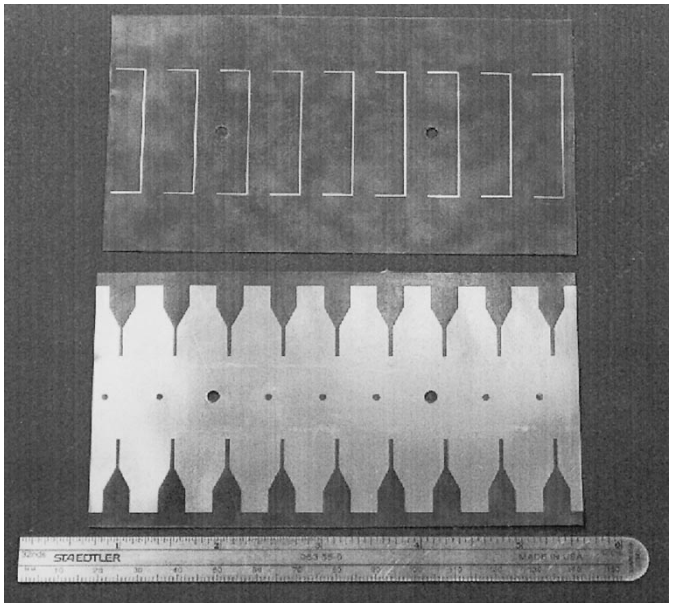

Fig. 1. Nine pairs of notch antennas (bottom) connected by striplines (top) to form a portion of a back-to-back array.

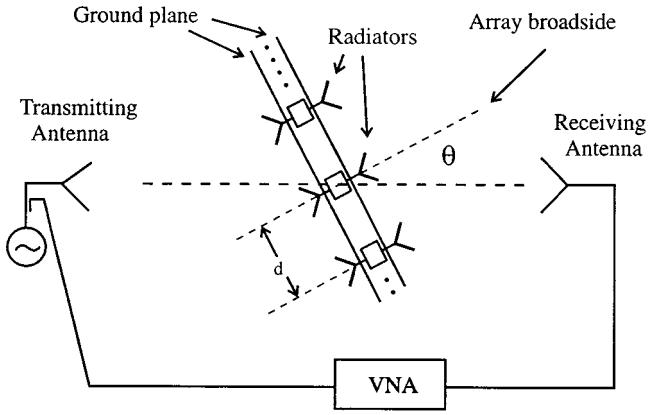

Fig. 2. Schematic sketch of free-space finite array measurement.

the transmission networks that connect the two faces of the lens are *identical* for all pairs of elements so that the "lens" *does not refocus* the incidence wavefront. The measurement is performed by placing the array to be tested between a pair of antennas and determining the transmission coefficient for the array-network-array lens. Measurement at any desired scan angle and frequency can be carried out with the angle of the lens and the frequency of the signal set to the desired values (see Fig. 2). The raw quantities being measured in the back-to-back technique are transmission coefficients, not reflection coefficients. In the measurement setup, the lens made of back-to-back antennas is inserted between the measuring ports of a vector network analyzer. The signal sent by one measuring port is picked up by the array on one side, relayed to the other side via the transmission network and re-radiated to the receiving port as illustrated in Fig. 2. It is *not necessary* to determine the absolute magnitude and phase of the transmission coefficient. Rather, only the ratio of the transmission coefficients for the "lenses" with different

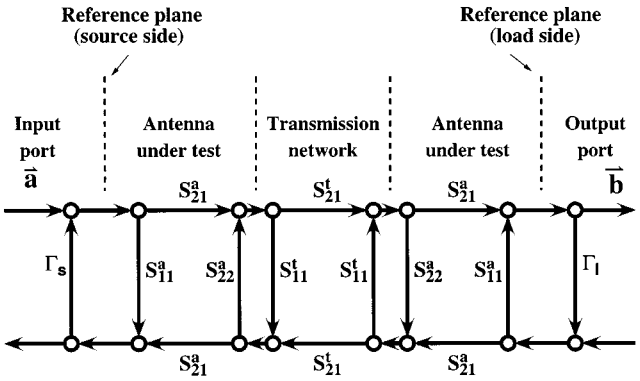

Fig. 3. Signal flow graph for back-to-back measurement.

transmission networks is needed to obtain the active impedance of the array elements.

The primary signal path through the lens is represented by the signal flow graph in Fig. 3. It models the antennas under test and the transmission network connecting them as two-port devices, with superscript a denoting antenna and t transmission network. For convenience, it is assumed that $S^a_{21} = S^a_{12}$, $S^t_{12} = S^t_{21}$, and $S^t_{11} = S^t_{22}$. This corresponds to a reciprocal antenna under test and a symmetric transmission network. This restriction can be removed, if necessary. The signal flow graph of Fig. 3 ignores leakage around the ground plane and other second-order effects. The derivation below also assumes a well-calibrated system ($\Gamma_s \approx \Gamma_l \approx 0$.). Some of the most important effects of those assumptions are discussed in Section IV.

If different transmission networks, $i = 1$ and 2, are used to construct two "lenses," the measured transmission coefficients can be expressed as

$$S^{mi}_{21} = \frac{S^a_{21} \cdot S^{ti}_{21} \cdot S^a_{21}}{1 - 2S^a_{22} \cdot S^{ti}_{11} + {S^a_{22}}^2 \cdot \left({S^{ti}_{11}}^2 - {S^{ti}_{21}}^2\right)}. \quad (1)$$

S^a_{22} is the reflection coefficient of the antenna seen by a transmission line. Two independent equations are necessary to solve for the unknowns $(S^a_{21} \cdot S^a_{12})$ and S^a_{22}, in (1).

With the assignment

$$R \equiv \frac{S^{m1}_{21} \cdot S^{t2}_{21}}{S^{m2}_{21} \cdot S^{t1}_{21}} = \frac{1 - 2S^a_{22} \cdot S^{t2}_{11} + {S^a_{22}}^2 \cdot \left({S^{t2}_{11}}^2 - {S^{t2}_{21}}^2\right)}{1 - 2S^a_{22} \cdot S^{t1}_{11} + {S^a_{22}}^2 \cdot \left({S^{t1}_{11}}^2 - {S^{t1}_{21}}^2\right)} \quad (2)$$

we have

$$\left[R \cdot \left({S^{t1}_{11}}^2 - {S^{t1}_{21}}^2\right) - \left({S^{t2}_{11}}^2 - {S^{t2}_{21}}^2\right)\right] \cdot {S^a_{22}}^2 - \left[R \cdot 2\left(S^{t1}_{11} - S^{t2}_{11}\right)\right] \cdot S^a_{22} + R - 1 = 0. \quad (3)$$

This is a quadratic equation of the unknown antenna reflection coefficient, S^a_{22}. All other quantities in (3) are known from either the measurements or from the knowledge of the transmission networks. In general, there will be two solutions to the quadratic equation (3). It is not possible to select the true solution without other information. This ambiguity can be removed by using a third known transmission network.

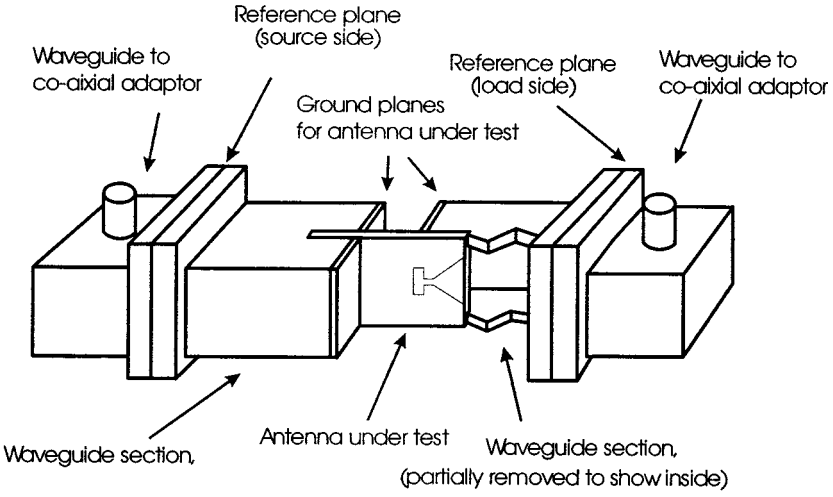

Fig. 4. Waveguide simulator measurement.

A. Waveguide Simulator

Notch antenna measurements in a waveguide simulator were performed by using the one-port looking-out method and the back-to-back scheme. Fig. 4 shows the setup for the back-to-back measurement in a waveguide simulator.

B. Free-Space Finite Arrays

The back-to-back measurement method was developed primarily to treat large scanning phased arrays, where mutual coupling is vitally important to array performance, but the cost to fabricate the feed networks required to test the array under all scan conditions is prohibitive. With this objective in mind, the back-to-back measurement method assumes that the cumulative behavior of elements in a finite array under test is close to that of an infinite array. This is a common assumption in phased-array analysis and it is valid if truncation effects that change the impedance of edge elements have little effect on the overall performance of the array under test. Then, like the array under test depicted in Fig. 2, the array under test receives a plane wave at angle θ from one side and re-radiates a plane wave at angle θ on the opposite side. The phase delay $(2\pi/\lambda) * d * \sin\theta$ is preserved as the signals pass through the identical transmission networks. Thus, both arrays of the lens operate at the same scan angle and have the same input impedance. The arrays that were used in the experiments described below were comprised of 100 elements in a 10×10 array. The arrays were mounted in a ground plane of size 1.2 m $\times$ 2.4 m.

III. Measurement Results

A. LTSA in the Waveguide Simulator

One-port waveguide simulators have been used for decades to help design large phased arrays and have proven to be successful [5]–[8]. On the other hand, back-to-back waveguide simulators have the advantages of not having to deal with the troubles associated with feed networks needed for multi-element simulators and with de-embedding transitions between different types of transmission media. Linearly tapered slot antennas (LTSA) (Fig. 5) were measured in both configurations to validate the back-to-back measurement scheme. The measured data are shown in Fig. 6 along with theoretical calculations obtained using a code similar to the one described in [17].

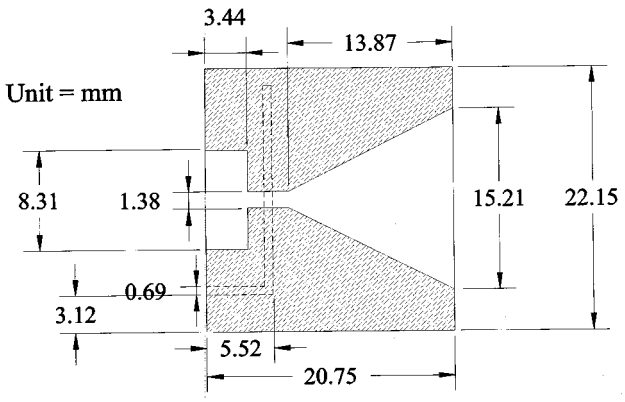

Fig. 5. LTSA measured in the waveguide simulator. Substrate = RT Duroid 5880 ($\epsilon_r = 2.2$, total thickness = 1.016 mm.)

In the one-port measurement, the effects of the coaxial-to-stripline adaptor must be removed by a custom-made thru-reflection-line (TRL) calibration kit. The deviation of the one-port measurement result from the other two is probably due to the imperfection in the de-embedding procedure.

B. Free-Space Finite Arrays

A 10×10 broken linearly tapered slot antenna (BLTSA) array was measured in an anechoic chamber using the setup depicted in Fig. 2. The dimensions of an array element are shown in Fig. 7. The measured impedance of the singly polarized array at broadside as well as scanning angles in the *E*-plane and *H*-plane are shown in Figs. 8 to 10. Also shown are computations using an infinite array computer model. Measured and computed impedances agree reasonably well, although some effects from array truncation to 100 elements and from measurement phenomena are evident.

Fig. 10, the computational result shows a scan blindness at 9.56 GHz, indicated by the "X" sign. The measured impedance also has a rather peculiar loop at this frequency. However, the

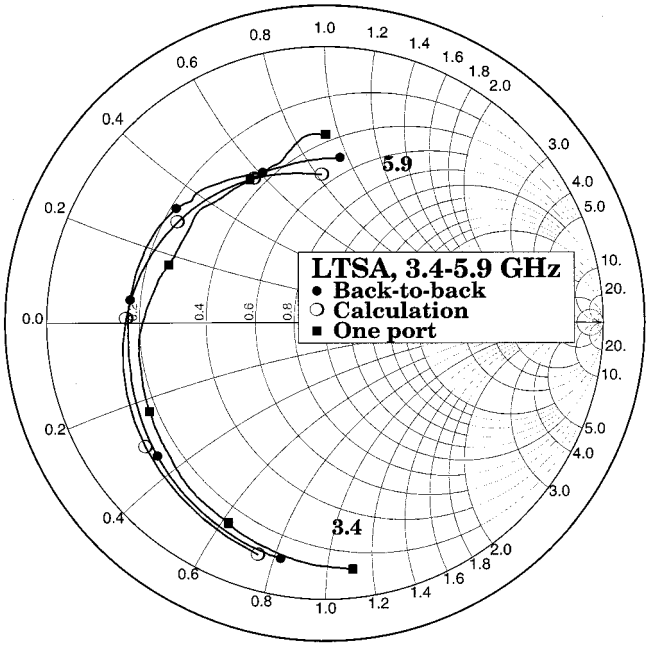

Fig. 6. Impedance of LTSA measured in the waveguide simulator. Frequency markers at 0.5 GHz intervals.

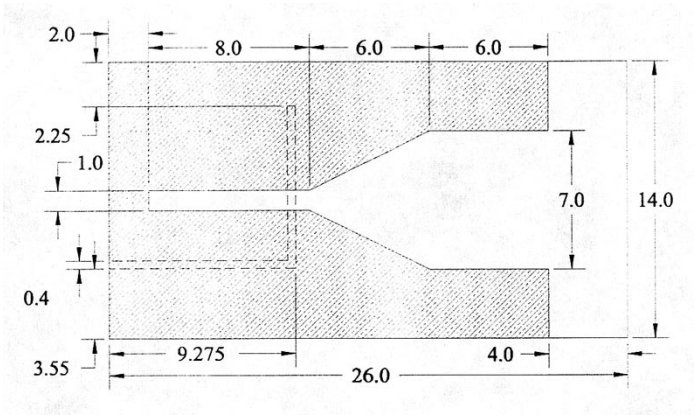

Fig. 7. Broken linearly tapered slot antenna measured in 10×10 finite arrays. Substrate = RT Duroid 5880 ($\epsilon_r = 2.2$) of 0.508 mm total thickness (unit = mm).

shape of the measured locus, differs from the computations at the scan blindness. This difference is discussed in Section IV.

IV. Error Analysis

Through experience gained by using the back-to-back measurement method and through analysis of the equations that represent the measured quantities and the calculated impedance some of the main sources of error have been identified.

A. Nonperfect Calibration

The most significant source of error in the waveguide simulator is imperfect calibration resulting in an impedance mismatch at the reference planes (Figs. 3 and 4). In the signal flow graph (Fig. 3) Γ_s and Γ_l represent these mismatches.

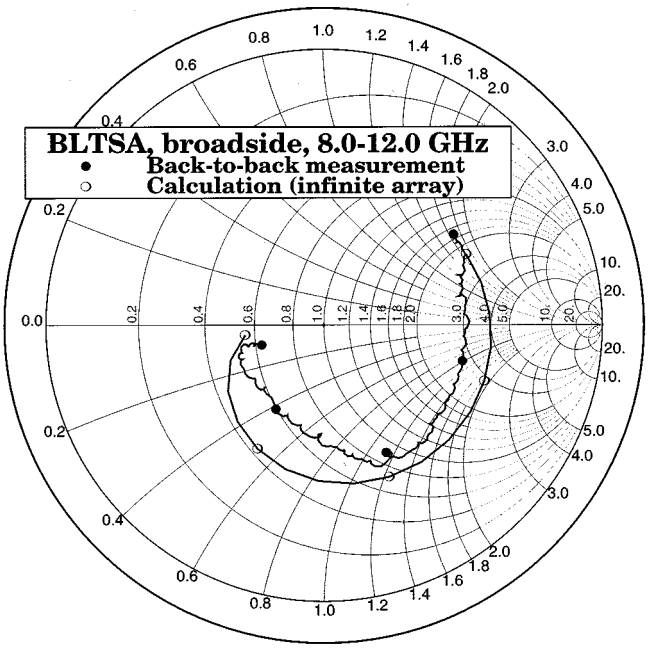

Fig. 8. Impedance of BLTSA at broadside. Frequency markers at 1 GHz intervals.

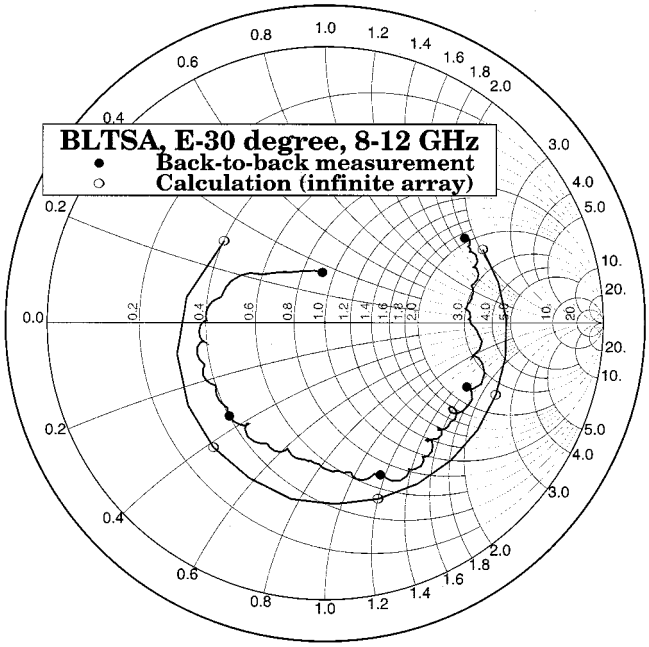

Fig. 9. Impedance of BLTSA at *E*-plane 30°.

Including the effects of Γ_s and Γ_l in the signal flow graph analysis leads to a generalized expression for the measured S_{21}

$$S_{21}^{mg} = \frac{S_{21}^{a} \cdot S_{21}^{t} \cdot S_{12}^{a}}{1 - D1 + D2 - D3 + D4} \tag{4}$$

where D1–D4 are listed in the Appendix.

Comparison of (1) and (4) reveals that the denominator of (4) is equal to the denominator of (1) plus several terms involving Γ_l and Γ_s. If the values of Γ_s and Γ_l both approach zero, (4)

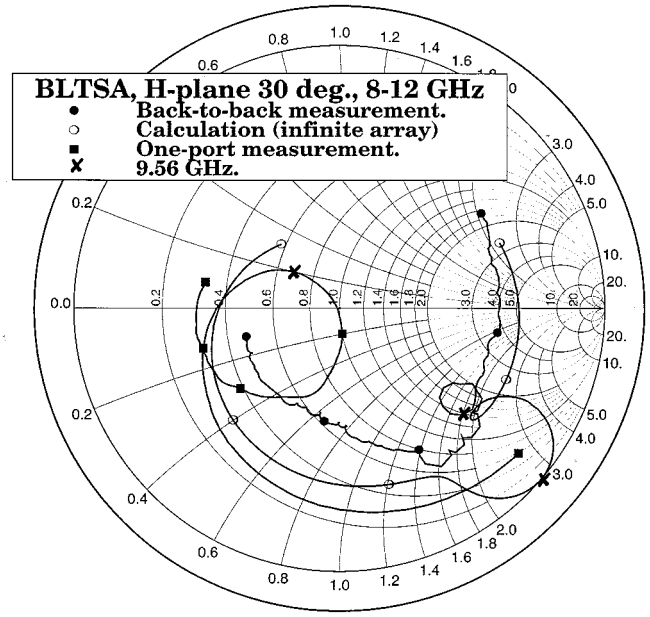

Fig. 10. Impedance of BLTSA at *H*-plane 30°.

reduces to the much simpler form of (1). In practice, the magnitudes of Γ_s and Γ_l could be as small as 0.01 (return loss of 40 dB) in a well-calibrated system. In cases where $|S^a_{22}| > 0.1$, those terms containing either Γ_l or Γ_s can be safely ignored since they are at least an order of magnitude smaller than the four dominate terms that appear in (1). However, when the antenna under test is well matched to the system impedance (i.e., $|S^a_{22}|$ approaches zero) and $|\Gamma_s|$, $|\Gamma_l|$ are close to or larger than $|S^a_{22}|$, those extra terms are no longer negligible. It has been shown [18] that antennas that are well matched to the measurement system impedance are more vulnerable to measurement errors. This is because the desired quantity, S^a_{22}, can only be extracted from the changes it causes to the directly measured transmission coefficients S^m_{21}. If the perturbation caused by the antenna under test is very small, its effect will easily be masked by the reflections from imperfect calibration.

B. Highly Mismatched Antennas and Resonant Circuits

Because the raw quantity measured is the transmission coefficient, the back-to-back measurement is not reliable when the transmitted signal is too small for adequate signal-to-noise ratio. This can happen when the antenna under test is poorly matched and not letting much of the signal through. In (1), this is understood as $|S^a_{21}| \sim 0$. Even if $|S^a_{21}|$ is not small enough to cause problems alone, there are still cases where the denominator of (1) approaches zero for some combination of S^a_{22} and the S-parameters of the transmission network. These difficulties can be identified *a posteriori*, but cannot be corrected unless a new transmission network is employed in the experiment. Fortunately, these difficulties occur only when the antenna is very poorly matched ($|S^a_{22}|$ near unity and $|S^a_{21}|$ small). For array design, it is usually sufficient to know that the antenna is very poorly matched.

C. Edge Effect Amplifies Errors at Scan Blindness

The finite-array back-to-back measurement relies upon the assumption that the cumulative behavior of the elements in the finite array under test will be similar to that of elements in an infinite array. If so, the array elements can be represented by a single two-port device. In the finite array measurements reported here, a moderate sized (10×10) array was utilized to approximate the infinite array environment. Using arrays containing a larger number of elements will certainly improve the measurement accuracy. The measured transmission coefficient S^m_{21} can be considered as the vector sum of radiation from each of the 100 elements. The cumulative effect gives an indication of the active element impedance in an infinite array. This works relatively well as shown in Figs. 8 and 9 until a scan blindness is encountered (Fig. 10). Under these anomalous conditions, elements in the central part of the array (which we want to see) behave like those in an infinite array and let very little signal go through. Their contributions to the measured transmission coefficient S^m_{21} are small. The measured S^m_{21} is then dominated by elements on the array edges, which experience truncation effects and do not behave the same as interior elements of a large array. The observed behavior of the finite array then differs significantly from the expectations for an infinite array, as seen in Fig. 10. To further explore this, the input impedance of an isolated BLTSA was measured. Fig. 10 shows that an isolate element has very different characteristics from those of central elements. Although edge elements of the array may not behave like isolated elements, they certainly will not behave like central elements. Thus, the measurements observed at a scan blindness of the infinite array (e.g. 9.56 GHz at *H*-plane 30°) are greatly "contaminated" by its edge elements. The 10×10 array impedance derived from the back-to-back measurements is closer to the center of the Smith chart as for the isolated element than it would be for the infinite array.

The existence of scan anomalies may not be immediately obvious from the derived antenna reflection coefficients, as in Fig. 10, but can be identified by checking the measured transmission coefficient S^m_{21}. For instance, the magnitude of S^m_{21} scanning at *H*-plane 30° show a dip of more than 10 dB around 9.56 GHz for antennas with both transmission networks. Yet the processed input impedance indicates better matched antennas for this scanning condition. Discrepancies like this should be enough to warn antenna designers about the possibility of scan anomalies. It is likely that measurements at scan blindness will always be dominated by edge elements, so the back-to-back method for finite arrays can be expected only to show some form of anomalous behavior, but not to yield an accurate estimate of infinite array impedance at a blindness. However, antenna designers usually need only to know if and where the anomaly occurs. The exact impedance at the anomaly is not important because the array is unusable there.

D. Leakage

Ideally, the measured transmission coefficient S^m_{21} should contain only the radiation relayed by the antennas under test. Measurements of finite arrays can be corrupted by leakage

around the ground plane. The measurement setup illustrated in Fig. 2 should illuminate the array under test with a uniform plane wave and it should not allow a significant signal to reach the receive antenna by any path except through the array. The 10×10 array tests reported here were performed with a ground plane that was approximately 1.2 m $\times$ 2.4 m. For broadside incidence, the leakage signal was about 20 dB below the signal transmitted through the array. However, when the incident angle is scanned by rotating the array and ground, as depicted in Fig. 2, the projected area of the ground plane decreases, allowing more signal to leak around the edges. The use of a near-field collimating source with sharp rolloff of the signal strength outside the area of the array could improve this aspect of measurement scheme, but leakage is expected to limit the scan range that can be measured unless specialized equipment is designed.

V. Conclusion

A back-to-back impedance measurement method is described. Results from the new method were validated by comparing to those from traditional waveguide simulator measurements and from numerical simulation.

The new test method can reduce the cost to develop and test a phased-array antenna by eliminating the feed network, while allowing full characterization of the array at all frequencies and scan angles. Since the feed network is not essential in characterizing the radiating aperture, eliminating it reduces the cost and simplifies the de-embedding procedure. This is especially useful when the antenna under test is not directly compatible with commonly available test equipment. The notch antennas examined in this paper are good examples as their natural feed structure—stripline cannot be connected directly to the VNA. The back-to-back method is very general, however, and can be used for other types of array elements. The measurement requires fabrication of two "lenses" comprised of input and output arrays and interconnecting transmission networks. This will be more expensive than fabricating a single array face, but the elimination of connectors and the feed network can significantly reduce cost and development time, especially if the arrays and transmission networks are fabricated by printed circuit techniques as in the examples presented here. There is no requirement for symmetry of the array elements, as in a waveguide simulator, so the method can be used when the only alternative is a fully configured array with feed network.

The back-to-back measurement utilizes transmission coefficients to extract the antenna impedance so the quality of the results will not be good if the antenna under test is poorly matched, resulting in a small signal-to-noise ratio at the receiver. Leakage around the ground plane corrupts the measurement especially at large scan angles, unless very large or specialized test fixtures are utilized. Also, the results for well matched antennas are more sensitive to measurement errors than those for antennas with a moderate mismatch. This annoyance can be overcome by using transmission networks with a different characteristic impedance that creates a moderated mismatch when the antenna achieves its desired impedance.

In addition to the cost savings of the new method, it offers the ability to test an array under a variety of scan conditions, frequencies, and polarizations. It is only necessary to orient the antenna under test and adjust the frequency of the signal to the desired values. The method has been implemented in an existing anechoic chamber as a removable ground plane into which the arrays are inserted. An ordinary vector network analyzer is used to measure the transmission coefficients and off-line data processing yields the antenna impedance. The method has been very useful for characterizing many types of printed antenna arrays and can be applied to other types of radiators.

Appendix

Terms appearing in generalized expression for the measured S_{21} with imperfect matching at the reference planes.

$$
\begin{aligned}
D1 =& 2S_{22}^{a}S_{11}^{t} + {S_{21}^{t}}^{2}{S_{22}^{a}}^{2} + \Gamma_s S_{11}^{a} + \Gamma_l S_{11}^{a} + \Gamma_s {S_{21}^{a}}^{2} S_{11}^{t} \\
&+ \Gamma_s {S_{21}^{a}}^{2}{S_{21}^{t}}^{2} S_{22}^{a} + \Gamma_s {S_{21}^{a}}^{2}{S_{21}^{t}}^{2}{S_{21}^{a}}^{2}\Gamma_l \\
&+ S_{22}^{a}{S_{21}^{t}}^{2}{S_{21}^{a}}^{2}\Gamma_l + S_{11}^{t}{S_{21}^{a}}^{2}\Gamma_l \\
D2 =& \Gamma_s S_{11}^{a} \cdot \left(2S_{22}^{a}S_{11}^{t} + S_{11}^{a}\Gamma_l + {S_{22}^{a}}^{2}{S_{21}^{t}}^{2}\right. \\
&\left. + S_{22}^{a}{S_{21}^{t}}^{2}{S_{21}^{t}}^{2}\Gamma_l + S_{11}^{t}{S_{21}^{a}}^{2}\Gamma_l\right) + {S_{22}^{a}}^{2}{S_{11}^{t}}^{2} \\
&+ S_{22}^{a}S_{11}^{t} \cdot \left(S_{11}^{a}\Gamma_l + S_{11}^{t}{S_{21}^{a}}^{2}\Gamma_l\right) + S_{11}^{t}S_{22}^{a}S_{11}^{a}\Gamma_l \\
&+ \Gamma_s {S_{21}^{a}}^{2}S_{11}^{t} \cdot \left(S_{11}^{t}S_{22}^{a} + S_{11}^{a}\Gamma_l + S_{11}^{t}{S_{21}^{a}}^{2}\Gamma_l\right) \\
&+ \Gamma_s {S_{21}^{a}}^{2}{S_{21}^{t}}^{2}S_{22}^{a}S_{11}^{a}\Gamma_l \\
D3 =& \Gamma_s S_{11}^{a}S_{22}^{a}S_{11}^{t} \cdot \left(S_{11}^{t}S_{22}^{a} + S_{11}^{a}\Gamma_l + S_{11}^{t}{S_{21}^{a}}^{2}\Gamma_l\right) \\
&+ \Gamma_s {S_{11}^{a}}^{2}S_{22}^{a}S_{11}^{t}\Gamma_l + \Gamma_s {S_{21}^{a}}^{2}S_{11}^{t}S_{11}^{t}S_{22}^{a}S_{11}^{a}\Gamma_l \\
&+ {S_{22}^{a}}^{2}{S_{11}^{t}}^{2}S_{11}^{a}\Gamma_l \\
D4 =& \Gamma_s {S_{11}^{a}}^{2}{S_{22}^{a}}^{2}S_{11}^{t}\Gamma_l.
\end{aligned}
$$

References

[1] L. Stark, "Microwave theory of phased-array antennas—A review," *Proc. IEEE*, vol. 62, pp. 1661–1701, Dec. 1974.

[2] N. Amitay, V. Galindo, and C. P. Wu, *Theory and Analysis of Phased Array Antennas*. New York: Wiley, 1971.

[3] R. J. Mailloux, "Phased-array theory and technology," *Proc. IEEE*, vol. 80, pp. 246–291, Mar. 1982.

[4] E. Brookner, "Radar of the 80s and beyond," in *Proc. IEEE Electro 84*, May 1986, session 4.

[5] P. W. Hannan, P. J. Meier, and M. A. Balfour, "Simulation of phased array antenna impedance in waveguide," *IEEE Trans. Antennas Propagat.*, vol. AP-11, pp. 715–716, Nov. 1963.

[6] P. W. Hannan and M. A. Balfour, "Simulation of phased array antenna in waveguide," *IEEE Trans. Antennas Propagat.*, vol. AP-13, pp. 342–353, May 1965.

[7] H. A. Wheeler, "A survey of the simulator technique for designing a radiating element in a phased-array antenna," in *Symp. Dig. Phased-Array Antenna Symp.*, vol. AP-13, Farmingdale, NY, June 1970, pp. 56–59.

[8] J. J. Gustincic, "The determination of active array impedance with multielement waveguide simulators," *IEEE Trans. Antennas Propagat.*, vol. AP-20, pp. 589–595, Nov. 1972.

[9] R. C. Hansen, Ed., *Microwave Scanning Antennas, Vol. II*. New York: Academic, 1966.

[10] W. K. Kahn, "Active reflection coefficient and element efficiency in arbitrary antenna arrays (Commun.)," *IEEE Trans. Antennas Propagat.*, vol. AP-17, pp. 653–654, Aug. 1969.

[11] D. M. Pozar, "The active element pattern," *IEEE Trans. Antennas Propagat.*, vol. 42, pp. 1176–1178, Aug. 1994.

[12] L. Schwartzman, "Analysis of phased array lenses," *IEEE Trans. Antennas Propagat.*, vol. AP-16, pp. 628–632, Nov. 1968.
[13] R. Chu, K. Lee, and M. Wong, "A network model of a feedthrough phased array lens of printed dipole elements," *IEEE Trans. Antennas Propagat.*, vol. AP-34, pp. 1410–1417, Dec. 1986.
[14] P. J. Rainville, "Investigation of SHF FET amplifiers in coplanar waveguide," Master's thesis, Univ. Massachusetts, Amherst, 1986.
[15] D. Rubin, "De-embedding mm-wave MIC's with TRL," *Microwave J.*, pp. 141–150, June 1990.
[16] D. H. Schaubert, W. Chang, and G. J. Wunsch, "Measurement of phased array performance at arbitrary scan angles," in *Proc. 1994 Antenna Applicat. Symp.*, Allerton Park, Monticello, IL, Sept. 1994.
[17] D. H. Schaubert, J. A. Aas, M. E. Cooley, and N. E. Buris, "Moment method analysis of infinite stripline-fed tapered slot antenna arrays with a ground plane," *IEEE Trans. Antennas Propagat.*, vol. 42, pp. 1161–1166, Aug. 1994.
[18] W. Chang, "A new method for measuring phased array antennas," Master's thesis, Univ. Massachusetts, Amherst, 1997.

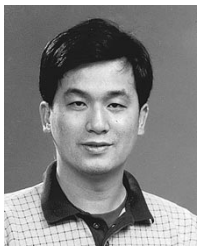

Wei-Chun Chang was born in Peng-Hu, Taiwan, R.O.C., on March 25, 1967. He received the B.S.E.E. degree from the National Taiwan University, Taipei, Taiwan, in 1989, and the M.S. degree in electrical and computer engineering from the University of Massachusetts, Amherst, in 1997. He is currently working toward the Ph.D. degree at University of Massachusetts, Amherst.

From 1991 to 1992, he was a Research Assistant and involved in building interfaces between medical sensors and personal computers at the Institute of Biomedical Engineering, National Yang-Ming Medical College, Taipei, Taiwan. He is now a Research Assistant at Antenna Laboratory, University of Massachusetts, Amherst. His current research interests include microstrip antennas, low-profile antennas, and antenna measurements.

Gregory J. Wunsch (S'89–M'96) received the B.S. and M.S.E.E. degrees from the University of Wisconsin, Milwaukee, in 1983 and 1991, respectively, and the Ph.D. degree in electrical engineering from the University of Massachusetts, Amherst in 1997.

He is currently with Sanders, A Lockheed Martin Company, Nashua, NH, as a Principal Electrical Engineer in the Antenna and Receivers Technology Department. In 1984, he joined the Boeing Company, where he was a Product Systems Engineer, performing troubleshooting for avionics systems. From 1988 to 1991, he was with the University of Wisconsin, Milwaukee, as a Research Assistant and began specializing in electromagnetic engineering. In the summer of 1989, he worked at the Mayo Foundation, Rochester, MN, where he developed computer programs for calculating crosstalk and signal transmission. From 1991 to 1999, he worked as Research Assistant and Postdoctoral Research Associate at the University of Massachusetts, Amherst. His research interests include antenna analysis and design and computational electromagnetics.

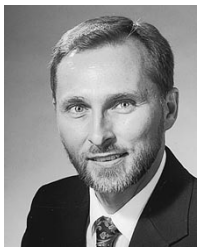

Daniel H. Schaubert (S'68–M'74–SM'79–F'89) has been with the University of Massachusetts since 1982 and is currently a Professor of electrical and computer engineering. Prior to joining the faculty at the University of Massachusetts, he was Lead Scientist the analysis of electromagnetic problems at the National Center for Devices and Radiological Health, Rockville, MD, and he was a Research Engineer at the Harry Diamond Laboratories near Washington, DC. He coedited *Microstrip Antennas*, (New York: IEEE Press, 1995).

Dr. Schaubert has been active in the IEEE Antennas and Propagation Society including President, Vice President, two terms on the Administrative Committee, Secretary-Treasurer, Newsletter Editor, Distinguished Lecturer Program Coordinator, Associate Editor of the Transactions, and IEEE Antennas and Propagation Society annual symposiums. He also organizes the annual Antenna Applications Symposium.